Microresonator soliton dual-comb imaging

Chengying Bao,* Myoung-Gyun Suh,* and Kerry Vahala†
T. J. Watson Laboratory of Applied Physics, California Institute of Technology, Pasadena, California 91125, USA.
*These authors contributed equally to this work.
†Corresponding author: vahala@caltech.edu

Fast-responding detector arrays are commonly used for imaging rapidly-changing scenes. Besides array detectors, a single-pixel detector combined with a broadband optical spectrum can also be used for rapid imaging by mapping the spectrum into a spatial coordinate and then rapidly measuring the spectrum. Here, broadband optical frequency combs generated from high-Q silica microresonators are used to implement this method. The microcomb is dispersed in two spatial dimensions to measure a test target. The target-encoded spectrum is then measured rapidly by multi-heterodyne beating with another microcomb having a slightly different repetition rate. The rapid image acquisition capability is also used to monitor the flow of microparticles in a fluid cell. This demonstration establishes that light sources and dual-comb detection methods for this form of rapid imaging can have a comparable chip-scale form factor to compact detector arrays.

I. INTRODUCTION

The development of the rapid-frame-capture detector array sensors based on CCD (charge-coupled device) and CMOS (complementary metal oxide semiconductor) technology has revolutionized imaging[1]. Also, by combining CCD/CMOS with streak cameras[2], frame rates of 100 billion per second are possible[3]. However, streak cameras are complicated and expensive systems. Moreover, high speed CCD/CMOS-based imaging encounters challenges such as compromised sensitivity at shorter exposure times, heat concentration, and on-chip storage memory and electronic readout speed[1,4]. As a result, there has been interest in alternative imaging methods. A recent approach uses the broadband spectrum of ultrashort optical pulses for fast imaging with a single-pixel detector (not an array)[5], and thereby avoids the above challenges for CCD/CMOS. The method works by mapping different optical frequencies of the broadband spectrum into distinct spatial locations using spatial dispersers such as demonstrated in the technique of femtosecond pulse shaping[6]. To create a 2-dimensional (2D) map, a conventional grating disperses the spectrum in one spatial dimension, while a virtually imaged phase array (VIPA) disperses light into the other spatial dimension. As shown in Fig. 1A, the grating and the VIPA create a '2D spectral shower' in which distinct optical frequencies have a one-to-one (spectral-spatial) correspondence with coordinates in 2-dimensions[5,7,8].

To recover the image, the spectrum can be measured by the time-stretch method, which converts the spectrally-encoded spatial information into a temporal waveform measured on a single-pixel photodetector[5]. This approach measures the image on a shot-by-shot basis and 6 MHz frame rates have been demonstrated[5]. As an alternative image recovery technique a dual-frequency-comb spectrometer has also been recently demonstrated[9]. This approach, termed here as dual-comb imaging, parallels the technique of dual-comb spectroscopy[10] by converting an optical spectrum into a low-bandwidth radio-frequency (RF) electrical signal. It can provide inteferometeric accuracy and precision for imaging. However, the demonstrated image acquisition rate is relatively low on account of the radio-frequency pulse rates of mode-locked fiber laser combs[9]. Also, line-scan spectral-spatial imaging using dual frequency combs has also been recently reported[11,12].

To generate broadband optical pulses for imaging, table-top, mode-locked lasers have so far been used. A recent advance in optical pulse generation and frequency comb generation is based on dissipative Kerr soliton mode locking in optical microcavities[13–16]. The devices provide high repetition rate soliton streams and their associated optical frequency combs feature smooth spectral envelopes. These miniature frequency combs or microcombs[17] are considered a possible way to dramatically reduce the form factor of conventional frequency comb systems. Accordingly, they are being studied for several applications including dual-comb spectroscopy[18,19], ranging[20,21], optical communications[22], optical frequency synthesis[23], and exoplant detection in astronomy[24,25]. Considering their possible application to the spectral-spatial imaging method, they offer not only a highly compact (chip-based) mode-locked optical pulse source, but, on account of their high pulse repetition rates, microcombs can increase image acquisition rates by several orders of magnitude when applied using the dual-comb heterodyne method. Also, the heterodyne method, when implemented using microcombs, avoids fiber optics required for the time-stretch image recovery method. As a result, a miniature system-on-a-chip is possible (dashed box in Fig. 1A). For these reasons, this work explores dual-comb imaging using soliton microcombs. The imaging method is demonstrated by measuring a test target and monitor-

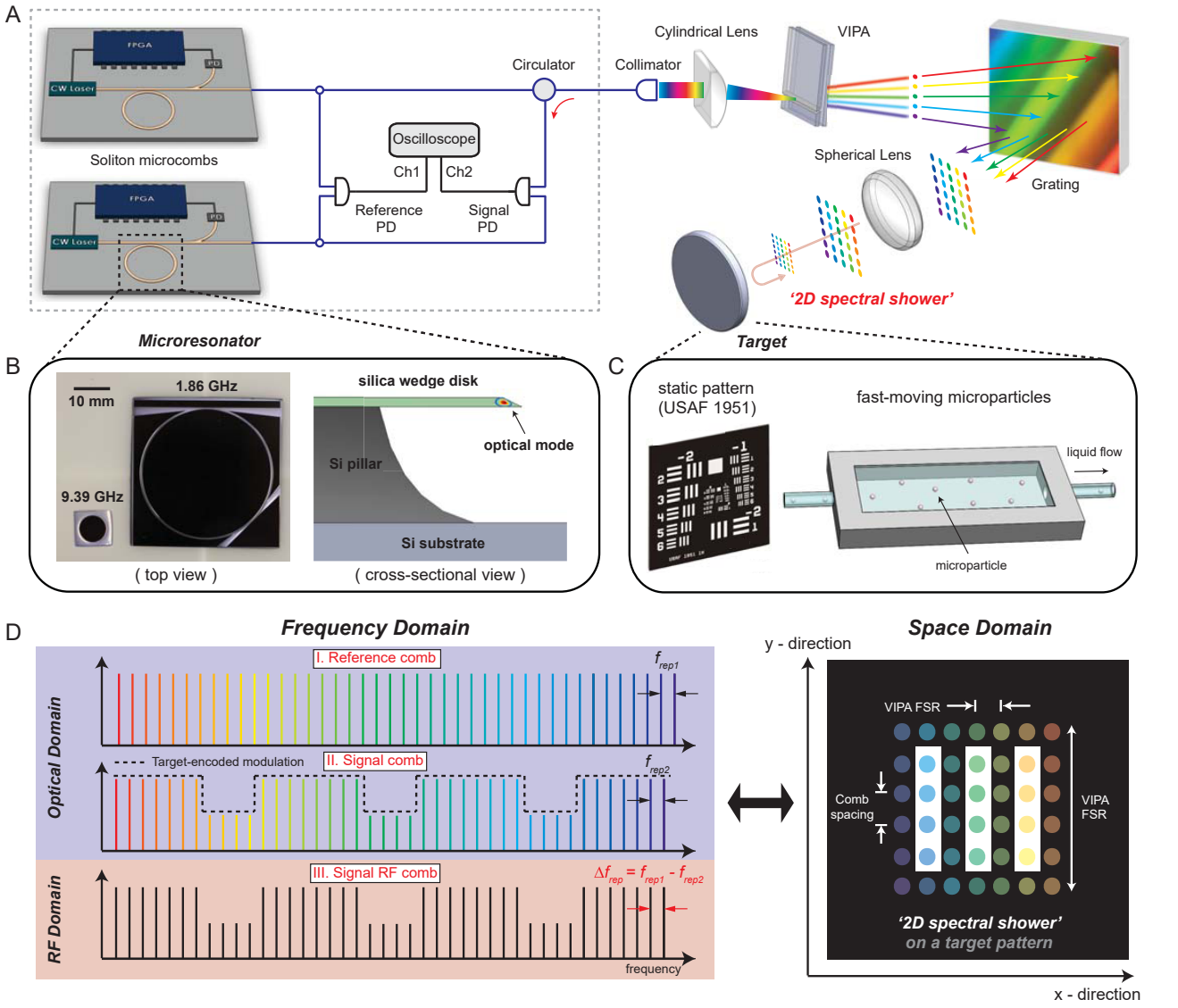

FIG. 1: **Dual-comb imaging using microresonator solitons** (A) A conceptual diagram showing the operational principle for spectral-spatial-mapping and rapid dual-microcomb imaging. Two soliton microcombs (signal and reference) having slightly different repetition rates are generated using two on-chip microresonators. A 2D disperser (VIPA+grating) maps frequencies from the signal microcomb into a 2D grid of spatial locations (spectral shower) that are reflected by a target. The reflected signal spectrum is measured by multi-heterodyne detection with the reference microcomb. (B) A photograph showing the top view of the two types of silica microresonators used in the experiment (left). The resonators have free-spectral ranges (FSRs) of 1.86 GHz and 9.39 GHz. A schematic cross-sectional view of the silica wedge microresonators with the spatial mode intensity indicated (right). (C) Measurement targets used include a USAF 1951 resolution chart and also microparticles within a flow-cell. (D) Spectral-spatial imaging proceeds by illuminating the target (right panel) with the 2D spectral shower formed as shown in panel A. As shown in the left panel, the target reflection amplitude is encoded onto the signal comb. The signal comb is then heterodyned with the reference comb to generate the RF comb. f_{rep1}, f_{rep2}, and Δf_{rep} are the frequency-line spacing of the reference comb, the signal comb, and the signal RF comb.

ing the flow of microparticles in a flow-cell (Fig. 1C). 200 kHz frame rates (5 μs integration time) are demonstrated which is over a 10,000-fold increase compared with prior heterodyne-based image recovery demonstrations using mode-locked fiber lasers[9].

II. RESULTS

Experimental setup. High-Q silica-on silicon wedge microresonators[26] with repetition rates of 1.86 GHz and 9.39 GHz[27] are used to generate the dual soliton streams.

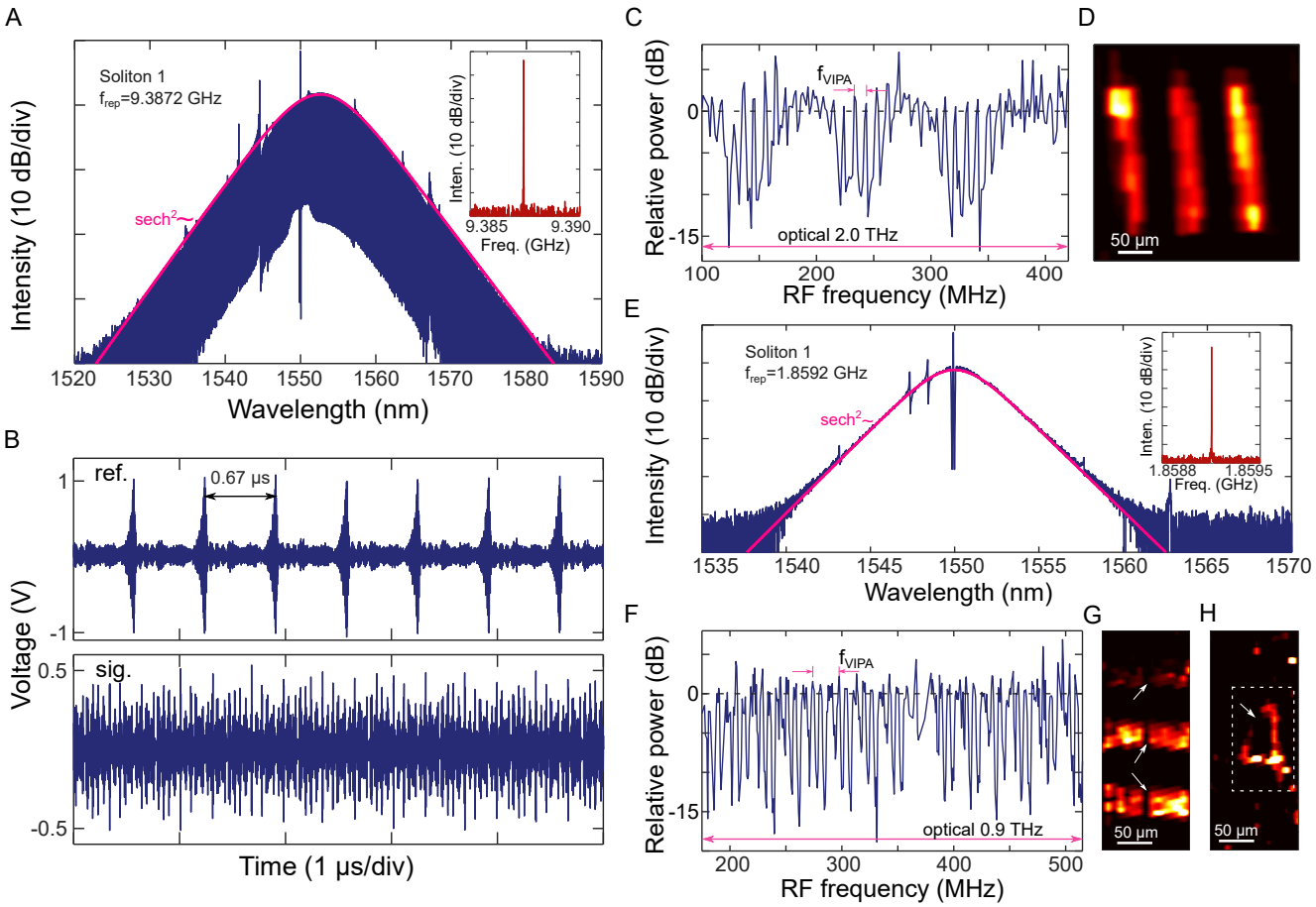

FIG. 2: **Dual-microcomb imaging of static targets.** (A) Typical optical spectrum of the 9.39 GHz soliton microcombs showing sech^2 spectral envelope fit as a red line. The inset is the electrical spectrum of the photodetected soliton pulse stream and gives the repetition rate. (B) An example of the measured interferogram in a 5 μs time window from the reference arm and the signal arm (see Fig 1A). (C) RF spectrum representing 3 vertical bars that are illuminated by the 9.39 GHz microcomb. The method to obtain this spectrum is described in the main text. The integration time used to obtain the spectrum is 5 μs. (D) Image of three vertical bars recontructed from the measured RF spectrum in panel C. (E) Typical optical spectrum of the 1.86 GHz soliton microcombs showing sech^2 spectral envelope fit as a red line. A notch near the spectral maximum is produced by a narrow-band filtering of the optical pump. The inset is the electrical spectrum of the photodetected soliton pulse stream. (F) RF spectrum representing 3 horizontal bars illumiated by the 1.86 GHz microcomb. The spectrum is obtained in the same way as panel C. (G) Image of 3 horizontal bars reconstructed from the measured RF spectrum in panel F. (G) Image of number '4' on the USAF target produced using the 1.86 GHz microcombs. The dark discontinuity shown by the arrows in (G, H) results from the spectral notch produced by filtering the optical pump (see panel E).

Images of the resonators are given in Fig. 1B and details on methods used to trigger and stabilize the soliton microcombs are presented elsewhere[14]. The microcombs are coupled directly to optical fibers using tapered-fiber couplers[28,29] and the signal comb and reference comb are conveyed along the optical train as shown in Fig. 1A. The VIPA and grating (600 lines/mm) act together to create the 2D spectral shower with the VIPA dispersing the spectrum along the vertical direction and the grating dispersing the spectrum along the horizontal direction. The VIPA disperses light only within its free-spectral-range (FSR) which means that optical frequencies ν and $\nu + m f_{\mathrm{VIPA}}$ (where m is an integer and f_{VIPA} is the VIPA FSR) will overlap in space. By adding a grating, frequencies ν and $\nu + m f_{\mathrm{VIPA}}$ can be further dispersed to create the 2D spectral shower as illustrated in Figs. 1A, D. The VIPA used in our experiment has an FSR of 60 GHz (LightMachinery) and this limits pixel count along the vertical direction to 32 pixels (1.86 GHz microcomb) and 6 pixels (9.39 GHz microcomb). Analysis of more optimal designs is provided in the Discussion. The spectral shower is reflected by the object, coupled back into the fiber for return to a photodetector where it is heterodyned with the reference microcomb. Fig. 1D illustrates

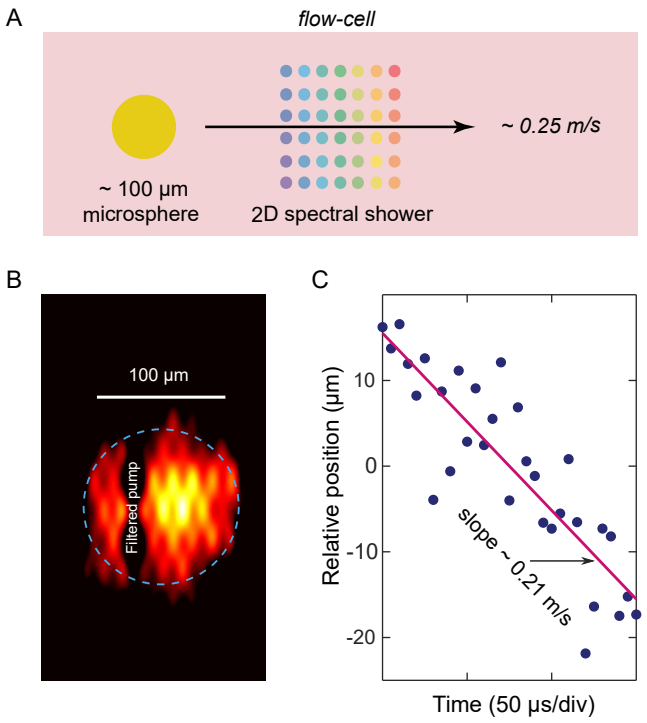

FIG. 3: **Monitoring flowing particles.** (A) An illustration of the microparticle monitoring experiment. Microparticles are suspended in water and flow inside the cell. When a particle passes through the 2D spectral shower, the particle can be imaged using the dual-comb interferogram. (B) A snapshot of a reconstructed microparticle. The dashed circle suggests the microparticle size (∼100 μm.). The dark vertical band results from filtering of the optical pump line. (C) Extracted center position of the microparticle versus time. A linear fit gives a flow velocity of 0.21 m/s in reasonable agreement with the set water flow velocity of 0.25 m/s.

how the image reflection amplitude is transferred from the spectral shower to the signal RF spectrum produced by dual-comb heterodyne.

Also shown in Fig. 1A are a collimator and a cylindrical lens (focal length of 150 mm) that focuses the collimated comb onto the VIPA. Additionally, the 2D spectral shower is focused onto the target by a spherical lens (focal length of 30 mm). In principle, the spherical lens can be replaced with two orthogonal cylindrical lenses so as to achieve independent control the 2D spectral shower along the two axes[7]. The targets are placed at the focal plane of the spherical lens and aligned to provide maximum reflection coupled into the fiber.

Imaging a static target. To demonstrate this approach, a USAF 1951 test target (negative) is imaged. Target patterns within Group 3 Element 4 of the target were illuminated. In a first measurement, two silica microcombs with repetition rates close to 9.39 GHz are used. The spectrum of one of the microcombs is shown in Fig. 2A and features a sech^2-shaped spectral envelope. The spectral spurs in the spectrum result from the dispersive wave emission induced by avoided-mode-crossings, which also assists single soliton generation[30]. The detected electrical spectrum for this comb is shown in the inset to Fig. 2A. The other microcomb has a similar spectrum, but its repetition rate differs from the first microcomb by ∼1.5 MHz. The close matching of repetition rates is possible by precise microfabrication control of the resonator diameters[26]. In Fig. 2B, typical examples of the heterodyned dual-comb interferograms measured over a 5 μs interval from the reference arm (upper panel) and signal arm (lower panel) are shown. While the reference interferogram contains a readily identifiable periodic signal resulting the difference in repetition rates of the signal and reference microcombs, the signal interferogram contains complex structure associated with the image.

To construct an image, an RF spectrum is first calculated by taking the fast Fourier transform (FFT) of the signal interferogram produced by illuminating a patterned region of the target and normalizing it by the FFT of the reference interferogram. Then, the same procedure is applied using a non-patterned (uniform) region of the target. Finally, the resulting normalized RF spectrum of the patterned region is further divided by the normalized RF spectrum of the non-patterned region to extract the target-encoded modulation, shown in Fig. 2C. The spectral lines with amplitudes larger than 0 dB might result from non-uniformity of the target (for example glints). These amplitudes, however, have a negligible affect on the resulting image because they represent small pixel values in the image (inverse reflectivity is used for reconstruction as a negative target is used). This 1D spectrum is sorted into a 2D matrix with each column being one VIPA FSR to recover the image (Fig. 2D). Both Fig. 2C and Fig. 2D should be compared with the spectrum and image in Fig. 1D. Some of the differences in the two cases result from the target in the actual experiment overlapping with multiple columns of the spectral shower as opposed to a single column as in Fig. 1D.

The granular-like features in the image result from the limited pixel number in the measurement (∼6×34). To illustrate improved resolution possible using a denser grid of pixels, two 1.86 GHz soliton microcombs were also tested in the imaging setup (see Fig. 2E for the optical and electrical spectrum of one of the microcombs). In this case, the pixel number in the vertical direction increases from 6 to 32 using the same 60 GHz VIPA and improved resolution results (see Fig. 2F and Fig. 2G for three horizontal bars). The increased pixel number in the vertical direction also enables resolution of the number '4' on the test target as shown in Fig. 2H. As an aside, the two 1.86 GHz soliton microcombs feature a Δf_{rep}=0.7 MHz, and Figs. 2G, H are recorded within a time interval of 10 μs.

Monitoring a flowing microparticle. The frame rate of the heterodyne image reconstruction approach is de-

termined by the requirement to just resolve the RF signal comb. Accordingly, because the electrical comb lines have a frequency separation equal to the difference in the repetition rates of the signal and reference soliton microcombs, this difference in repetition rates is close to the frame rate and can be quite high when using soliton microcombs.

To demonstrate measurement of a rapidly-changing scene, two 9.39 GHz soliton microcombs are used to monitor a microparticle moving in a high-speed flow-cell (Fig. 3A and Fig. 1C). For this purpose a $\sim$ 0.25 m/s laminar flow cell (cross section 0.2 mm $\times$ 8 mm) was set up and microparticles with diameter of $\sim$ 100 μm were suspended in water to flow through the cell. To improve signal-to-noise a mirror was placed behind the cell which has transparent surfaces. When a microparticle passes through the spectral shower, it modulates lines in the spectral shower. An image of a recorded flowing microparticle is shown in Fig. 3B. The size of the reconstructed microparticle (dashed circle in figure) is consistent with the particle actual size. The particles are not well resolved on account of the limited pixel number. To illustrate the measured motion of the microparticle, its center position is plotted versus time in Fig. 2C. A linear fit gives a flowing velocity of 0.21 m/s, consistent with the flow-cell set-point velocity of 0.25 m/s. A 200 kHz frame-rate was used in this measurement.

III. DISCUSSION

Because pixel count ($N \times M$) is equal to the number of microcomb lines, it follows that $N \times M = B/f_{\rm rep}$ where B is the microcomb bandwidth and $f_{\rm rep}$ is the microcomb repetition rate. Large comb bandwidths are therefore highly advantageous for improving resolution. Along these lines, dispersion engineering of the microresonator[31] or spectrally broadening the microcomb either through intracavity dipersive wave generation[32,33] or external (chip-based) broadeners[34] can provide octave-span spectral coverage. The assignment of these pixels to horizontal and vertical axes is controlled through the VIPA FSR ($f_{\rm VIPA}$) such that $N = f_{\rm VIPA}/f_{\rm rep}$ and $M = B/f_{\rm VIPA}$. For a square array ($N = M$) one must have $f_{\rm VIPA}^2 = Bf_{\rm rep}$. As examples, a 20 THz comb bandwidth ($\sim$1/6 of an octave at 1.55 μm) would enable a horizontal pixel number of 100 using a 200 GHz VIPA (custom design available at LightMachinery). For the vertical direction, the pixel number could be increased to over 107 (21) using the 1.86 GHz (9.39 GHz) microcombs. These should be compared to the existing spectral shower array dimensions of $\sim$32$\times$15 for the 1.86 GHz microcomb and $\sim$6$\times$34 for the 9.39 GHz microcomb.

Finally, there is a trade-off between the frame rate and pixel number given by by $N \times M < f_{\rm rep}/(2\Delta f_{\rm rep})$. This expression results from the need to avoid spectral folding of the RF comb lines. $\Delta f_{\rm rep}$ is related to the frame rate by $\Delta f_{\rm rep} = C f_{\rm frame}$ where C is the number of periods in the interferogram that must be intregrated to determine the signal and is set by signal-to-noise. In the present work, $C \sim 7$. Accordingly, this expression can also be written as follows: $N \times M \times C f_{\rm frame} < f_{\rm rep}/2$. Thus, an $N \times M$ =10,000 pixel spectral shower produced using an $f_{\rm rep}$ =1.86 GHz (9.39 GHz) microcomb, will provide a maximum frame rate of approximately 14 kHz (70 kHz). It is also possible to eliminate $N \times M$ in the above expressions to arrive at: $f_{\rm frame} < f_{\rm rep}^2/(2BC)$, which illustrates the importance of higher repetition rate to achieve higher frame rate, making microcombs attractive for this application.

Although not demonstrated here, the dual-comb method is a coherent measurement. As a result, phase information can also be retrieved, enabling acquisition of 3 dimensional information on the target[9]. For this purpose, the two combs must be phase locked with distinct repetition rates. Counter-propagating solitons within a single microresonator are accordingly a promising candidate for this coherent phase retrieval as they have high mutual coherence[35,36]. Finally, because the dual-comb measurement can resolve single comb lines, the spatial resolution is set by the imaging system only. This is in contrast to the time-stretch method where spatial resolution can also be limited by the ability to resolve the frequency components[5].

In summary, imaging using soliton microcombs has been demonstrated. Frame rates as high as 200 kHz enabled measurement of the high speed flow of microparticles. The current demonstration was in the 1.55 μm band, but can be readily shifted to the 1 μm band which could be more suitable for biological applications[37]. The method can find widespread applications in life science as well as in industrial production. For example, it could be a useful tool to study biochemical waves in cells[38] and for flow cytometry applications[39,40].

Acknowledgments The authors thank Taeyoon Jeon for helpful discussions on the flow-cell experiment. This work is supported by the Defense Advanced Research Projects Agency under the SCOUT program (award no. W911NF-16-1-0548), the Air Force Office of Scientific Research (award no. FA9550-18-1-0353) and the Kavli Nanoscience Institute. CB gratefully acknowledges support from a postdoctoral fellowship from the Resnick Institute, Caltech.

Author Contributions All the authors conceived the experiment, analyzed the data and wrote the manuscript. CB and MGS conducted the experiments under the supervision of KV.

Author Information Correspondence and requests for materials should be addressed to KV (vahala@caltech.edu).

[1] Kondo, Y. *et al.* Development of hypervision hpv-x high-speed video camera. *Shimadzu Rev* **69**, 285–291 (2012).

[2] Hamamatsu Photonics, K. Guide to streak camera. *Hamamatsu, Hamamatsu City Japan* (2010).

[3] Gao, L., Liang, J., Li, C. & Wang, L. V. Single-shot compressed ultrafast photography at one hundred billion frames per second. *Nature* **516**, 74 (2014).

[4] El-Desouki, M. *et al.* Cmos image sensors for high speed applications. *Sensors* **9**, 430–444 (2009).

[5] Goda, K., Tsia, K. & Jalali, B. Serial time-encoded amplified imaging for real-time observation of fast dynamic phenomena. *Nature* **458**, 1145 (2009).

[6] Weiner, A. M. Femtosecond pulse shaping using spatial light modulators. *Rev. Sci. Instr.* **71**, 1929–1960 (2000).

[7] Supradeepa, V., Huang, C.-B., Leaird, D. E. & Weiner, A. M. Femtosecond pulse shaping in two dimensions: Towards higher complexity optical waveforms. *Opt. Express* **16**, 11878–11887 (2008).

[8] Diddams, S. A., Hollberg, L. & Mbele, V. Molecular fingerprinting with the resolved modes of a femtosecond laser frequency comb. *Nature* **445**, 627 (2007).

[9] Hase, E. *et al.* Scan-less confocal phase imaging based on dual-comb microscopy. *Optica* **5**, 634–643 (2018).

[10] Coddington, I., Newbury, N. & Swann, W. Dual-comb spectroscopy. *Optica* **3**, 414–426 (2016).

[11] Wang, C. *et al.* Line-scan spectrum-encoded imaging by dual-comb interferometry. *Opt. Lett.* **43**, 1606–1609 (2018).

[12] Dong, X. *et al.* Ultrafast time-stretch microscopy based on dual-comb asynchronous optical sampling. *Opt. lett.* **43**, 2118–2121 (2018).

[13] Herr, T. *et al.* Temporal solitons in optical microresonators. *Nature Photonics* **8**, 145 (2014).

[14] Yi, X., Yang, Q.-F., Yang, K. Y., Suh, M.-G. & Vahala, K. Soliton frequency comb at microwave rates in a high-q silica microresonator. *Optica* **2**, 1078–1085 (2015).

[15] Joshi, C. *et al.* Thermally controlled comb generation and soliton modelocking in microresonators. *Opt. Lett.* **41**, 2565–2568 (2016).

[16] Wang, P.-H. *et al.* Intracavity characterization of microcomb generation in the single-soliton regime. *Opt. Express* **24**, 10890–10897 (2016).

[17] Kippenberg, T. J., Holzwarth, R. & Diddams, S. A. Microresonator-based optical frequency combs. *Science* **332**, 555–559 (2011).

[18] Suh, M.-G., Yang, Q.-F., Yang, K. Y., Yi, X. & Vahala, K. J. Microresonator soliton dual-comb spectroscopy. *Science* **354**, 600–603 (2016).

[19] Dutt, A. *et al.* On-chip dual-comb source for spectroscopy. *Science Advances* **4**, e1701858 (2018).

[20] Suh, M.-G. & Vahala, K. J. Soliton microcomb range measurement. *Science* **359**, 884–887 (2018).

[21] Trocha, P. *et al.* Ultrafast optical ranging using microresonator soliton frequency combs. *Science* **359**, 887–891 (2018).

[22] Marin-Palomo, P. *et al.* Microresonator-based solitons for massively parallel coherent optical communications. *Nature* **546**, 274 (2017).

[23] Spencer, D. T. *et al.* An integrated-photonics optical-frequency synthesizer. *Nature* **557**, 81 (2018).

[24] Obrzud, E. *et al.* A microphotonic astrocomb. *arXiv preprint arXiv:1712.09526* (2017).

[25] Suh, M.-G. *et al.* Searching for exoplanets using a microresonator astrocomb. *arXiv preprint arXiv:1801.05174* (2018).

[26] Lee, H. *et al.* Chemically etched ultrahigh-q wedge-resonator on a silicon chip. *Nature Photonics* **6**, 369 (2012).

[27] Suh, M.-G. & Vahala, K. Gigahertz-repetition-rate soliton microcombs. *Optica* **5**, 65–66 (2018).

[28] Cai, M., Painter, O. & Vahala, K. J. Observation of critical coupling in a fiber taper to a silica-microsphere whispering-gallery mode system. *Phys. Rev. Lett.* **85**, 74–77 (2000).

[29] Spillane, S. M., Kippenberg, T. J., Painter, O. J. & J., V. K. Ideality in a fiber-taper-coupled microresonator system for application to cavity quantum electrodynamics. *Phys. Rev. Lett.* **91**, 043902 (2003).

[30] Bao, C. *et al.* Spatial mode-interaction induced single soliton generation in microresonators. *Optica* **4**, 1011–1015 (2017).

[31] Yang, K. Y. *et al.* Broadband dispersion-engineered microresonator on a chip. *Nature Photonics* **10**, 316 (2016).

[32] Li, Q. *et al.* Stably accessing octave-spanning microresonator frequency combs in the soliton regime. *Optica* **4**, 193–203 (2017).

[33] Pfeiffer, M. H. *et al.* Octave-spanning dissipative kerr soliton frequency combs in si 3 n 4 microresonators. *Optica* **4**, 684–691 (2017).

[34] Lamb, E. S. *et al.* Optical-frequency measurements with a kerr microcomb and photonic-chip supercontinuum. *Phys. Rev. Appl.* **9**, 024030 (2018).

[35] Yang, Q.-F., Yi, X., Yang, K. Y. & Vahala, K. Counter-propagating solitons in microresonators. *Nature Photonics* **11**, 560–564 (2017).

[36] Joshi, C. *et al.* Counter-rotating cavity solitons in a silicon nitride microresonator. *Opt. Lett.* **43**, 547–550 (2018).

[37] Lee, S. H. *et al.* Towards visible soliton microcomb generation. *Nature Communications* **8**, 1295 (2017).

[38] Petty, H. R. High speed microscopy in biomedical research. *Optics and Photonics News* **15**, 40–45 (2004).

[39] Watson, J. V. *Introduction to flow cytometry* (Cambridge University Press, 2004).

[40] Goda, K. *et al.* High-throughput single-microparticle imaging flow analyzer. *Proc. Natl. Acad. Sci.* **109**, 11630–11635 (2012).